Automatic Brain Hemorrhage Segmentation and Classification in CTscan Images

Bahare Shahangian
Department of Electrical Engineering,
Najafabad Branch, Islamic Azad University,
Isfahan, Iran.

Hossein Pourghassem
Department of Electrical Engineering,
Najafabad Branch, Islamic Azad University,
Isfahan, Iran.
h_pourghasem@iaun.ac.ir

Abstract— **Brain hemorrhage detection and classification is a major help to physicians to rescue patients in an early stage. In this paper, we have tried to introduce an automatic detection and classification method to improve and accelerate the process of physicians' decision-making. To achieve this purpose, at first we have used a simple and effective segmentation method to detect and separate the hemorrhage regions from other parts of the brain, and then we have extracted a number of features from each detected hemorrhage region. We selected some of convenient features by using a Genetic Algorithm (GA)-based feature selection algorithm. Eventually, we have classified the different types of hemorrhages. Our algorithm is evaluated on a perfect set of CT-scan images and the segmentation accuracy for three major types of hemorrhages (EDH, ICH and SDH) obtained 96.22%, 95.14% and 90.04%, respectively. In the classification step, multilayer neural network could be more successful than the KNN classifier because of its higher accuracy (93.3%). Finally, we achieved the accuracy rate of more than 90% for the detection and classification of brain hemorrhages.**

Keywords—brain hemorrhage; segmentation; GA; neural network; KNN classifier

I. INTRODUCTION

Brain hemorrhage is the first cause of death in ages between 15-24, and the third after heart diseases and cancers in other ages. In most cases, the cause of death or disability of some body organs is that hemorrhages are diagnosed late or misdiagnosed. Saving the lives of such patients completely depends on detecting the correct location and type of the hemorrhage in an early stage. Generally, brain hemorrhages are divided into 5 main types: Epidural Hemorrhage (EDH) - Subdural Hemorrhage (SDH) –Subarachnoid Hemorrhage (SAH)-Intracerebral Hemorrhage (ICH) - Intraventricular Hemorrhage (IVH). In this study we have chosen EDH, SDH and ICH hemorrhages because in these types of hemorrhages the patients' lives entirely depend on their early diagnosis, particularly in ICH hemorrhages, in which the hemorrhage is in the brain tissue. The most common approaches used for brain hemorrhage segmentation and classification are: thresholding [1, 2, 3], active contour [4, 5], region growing technique [3, 4] and clustering techniques like fuzzy c-means algorithms [5]. Lauric and Frisken [2] used three soft segmentation methods: Bayesian Classification, Fuzzy C-Means (FCM) and Expectation Maximization (EM). Although those methods were able to segment brain and CSF in CT images, they were unable to distinguish gray matter from white matter.

Our aim in this paper is to introduce an independent detection and classification method to improve and accelerate the physicians' decision-making process. There are some challenges in detecting and classifying brain hemorrhages: (1) the existence of noise and excessive parts such as the skull, brain ventricles and soft tissue edema in brain CT images (2) the uncertain position of hemorrhage in some types (3) the similarity of shape and texture between some hemorrhage types (for example EDH and SDH occur with the same texture in the same intracranial space), which lead to extracting redundant or useless features and consequently to low classification accuracy.

In this paper, to overcome these disadvantages we have proposed an independent and automatic method that includes 4 steps: 1) Preprocessing and segmentation: in this step the noise, skull and brain ventricles are removed, then the hemorrhages are separated from other parts of the brain by using thresholding. 2) A number of features are extracted from each hemorrhage region, 3) the GA based feature selection is used to improve the classification accuracy, 4) in the last step we classified hemorrhages with two different classifiers. The rest of this paper is organized as follows. Section 2 explains principles of our proposed segmentation and classification brain hemorrhage structure. In section 3 the experimental results of the proposed structure is described and finally in section 4 the conclusions are presented.

II. PROPOSED BRAIN HEMORRHAGE SEGMENTATION AND CLASSIFICATION STRUCTURE

The block diagram of the proposed structure is shown in Fig. 1. In the segmentation step, after removing the skull and ventricles of the brain, median filter is used for de-noising the images. Then, we detect the hemorrhage regions from the CT brain images using thresholding. In the feature extraction step, for each hemorrhage region a number of features are extracted. After that, to improve the accuracy of classification quantifiable features are selected by using Genetic Algorithm

(GA) based feature selection. Lastly, the neural network classifier is used to classify the hemorrhage into different types according to the extracted features and then the KNN classifier is employed to compare the performance of two classifiers. The details of the proposed structure are obtained in the following.

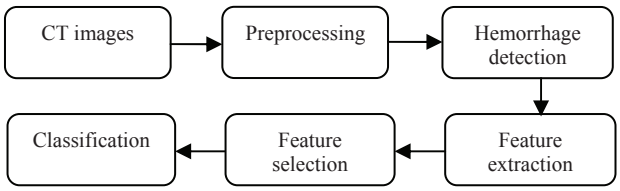

Fig. 1. Block diagram of the proposed structure

A. Segmentation

- Removing the Skull and Brain Ventricles

In the brain images, skull and brain ventricles, respectively, are in white and black color. In the histogram of these images three peaks exist. $P1$, the first peak, is expected to be the ventricles of the brain, while $P2$ may contain the object of interest, which is the brain, and the third peak, $P3$ that has the highest intensity, is expected to be the skull. So, the skull and brain ventricles were removed by suppressing (setting to zero) any pixels that are above 225 and below 100 in a gray scale map. Fig. 2 shows a CT scan brain image and its histograms before and after the skull and brain ventricles were removed.

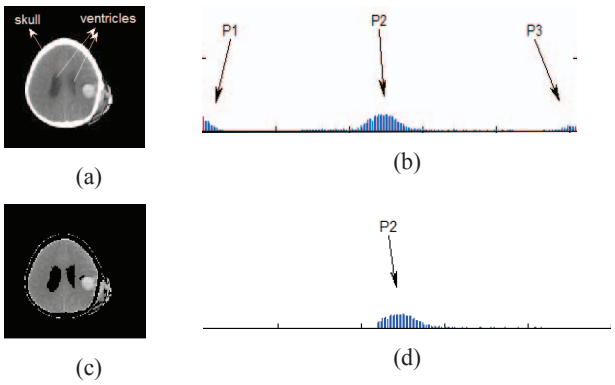

Fig. 2. *Original image b) histogram of original image c) image after remove the skull and ventricles d) histogram of c*

- Noise Reduction

After removing the skull and brain ventricles we are encountered with two other problems:1) the remaining lines where the skull has been removed, which can cause error in hemorrhage segmentation 2) the low quality of images because of the existing noise, which is solved with the image intensity adjustment and the use of median filter. The median filter is an effective method for noise reduction and it is a more robust method than the traditional linear filtering because it preserves the sharp edges.

- Soft Tissue Edema Removing

In some images, an additional part due to soft tissue edema is created outside the skull that may cause errors in segmentation, so we try to remove it. In order to do this, first we make a mask with the same size with the part of image that has the biggest area. Then, we multiply the mask by the image obtained from the previous step. Thus, this additional part becomes zero and is removed.

$$x(i,j)=\begin{cases}1 & for\ each\ (i,j)\ inside\ A\\ 0 & otherwise\end{cases}$$

where,

$$z(k,h)=x(i,j)\times y(m,n)=\begin{cases}y(m,n) & for\ each\ (i,j)\ inside\ A\\ 0 & otherwise(soft\ tissue\ edema)\end{cases}$$

where, $x(i,j)$ is the mask, A is the part of the original image that has the biggest area, $y(m,n)$ is the image obtained from the previous step and $z(k,h)$ is the image after removing the soft tissue edema.

- Hemorrhage Region Detection

After the previous steps, now according to the image intensity distribution we define an appropriate threshold, such that it could separate the hemorrhage region from other parts, and therefore a binary image based on this threshold containing the hemorrhage regions in white is generated. The middle results of our algorithm for detecting the brain hemorrhages are obtained in Fig. 3.

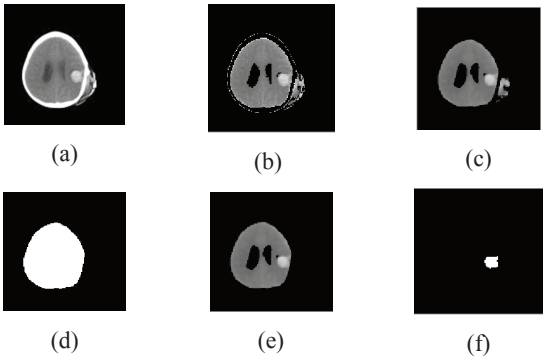

Fig. 3. a)original image b)image after remove the skull and ventricles c) image after noise reduction d)mask of the image e)image after remove the soft tissue edema f)detected hemorrhage

B. Feature Extraction:

The purpose of feature extraction is to reduce the original data set by measuring certain properties of features that distinguish input patterns [10]. Physicians use the position, shape, size and texture of the hemorrhage regions to classify and identify them. Therefore we need quantifiable features that describe the size, shape, texture and position of hemorrhage regions. We extract the following features from each hemorrhage region:

- Extracted Shape Features:

1. Area: the actual number of pixels in the hemorrhage region

2. Perimeter: the distance around the boundary of the hemorrhage region
3. Orientation: the angle between the x-axis and the major axis of the ellipse that has the same second-moments as the hemorrhage region.
4. Major axis length: The length (in pixels) of the major axis of the ellipse that has the same normalized second central moments as the hemorrhage region.
5. Minor axis length: The length (in pixels) of the minor axis of the ellipse that has the same normalized second central moments as the hemorrhage region.
6. Extent: The proportion of the pixels in the bounding box that are also in the hemorrhage region.
7. Convex area: Scalar that specifies the number of pixels in Convex Image
8. Solidity: The proportion of the pixels in the convex hull that are also in the hemorrhage region.

$$solidity = \frac{area}{convexarea} \quad (3)$$

9. Equivdiameter: Scalar that specifies the diameter of a circle with the same area as the hemorrhage region.

$$equivdiameter = \sqrt{4 \times \frac{area}{\pi}} \quad (4)$$

10. filled area: Scalar specifying the number of pixels in filled Image

- Extracted Texture Features:

1. Contrast: Returns a measure of the intensity contrast between a pixel and its neighbor over the whole image.

$$contrast = \sum_{i,j} (i-j)^2 p(i,j) \quad (5)$$

2. Energy: Returns the sum of squared elements in the GLCM (Gray-Level Co-Occurrence Matrix).

$$energy = \sum_{i,j} P(i,j)^2 \quad (6)$$

3. Correlation: Returns a measure of how correlated a pixel is to its neighbor over the whole image.

$$correlation = \sum_{i,j} \frac{(i-\mu_j)(j-\mu_j)P(i,j)}{\sigma_i \sigma_j} \quad (7)$$

Where

$$\mu_i = \sum_i i \sum_j P(i,j) \qquad , \mu_j = \sum_j j \sum_i P(i,j)$$

$$\sigma_j = \sum_j (j-\mu_j)^2 \sum_i P(i,j) \ , \sigma_i = \sum_i (i-\mu_i)^2 \sum_j P(i,j)$$

4. Homogeneity: Returns a value that measures the closeness of the distribution of elements in the GLCM matrix to the GLCM diagonal.

$$Homogeneity = \sum_{i,j} \frac{P(i,j)}{i+(i-j)} \quad (8)$$

C. *Feature selection and optimization using GA:*

The number of extracted features in the previous step can be quite large, irrelevant or redundant. Therefore we try to select the best ones with feature selection to improve classification accuracy. In this study, Genetic algorithm based feature selection was used to reduce features.

- Genetic Algorithm:

GA is an adaptive method of global-optimization searching. It is based on Darwin's fittest principle, which states that an initial population of individuals evolves through natural selection in such a way that the fittest individuals have a higher chance of survival [11].

Here, first the GA defines a population of weight vector w, where the size of each w is the size of the data pattern f, and then each w from the GA is multiplied with every sample's data pattern vector f, yielding a new feature vector m for the given data. The KNN algorithm then classifies the entire m data set and the results of the classification for a known training sample set are fed back as the fitness function, to guide the genetic algorithm. The fitness function:

$$fitness = w.e + \frac{w_{nb}}{N} \quad (10)$$

where, w is the weight vector of features, e is the classification error rate and w_{nb} is the weight of the N feature participated in the classification where $N \neq 0$ (The fitness function used in this study is the error rate of the KNN classifier) [12].

D. *Classification:*

In the classification step the input test images are classified into different classes of hemorrhage, to achieve this; two classification methods are used to compare the results to choose the best classifier.

- K-Nearest Neighbor (KNN) Algorithm:

KNN algorithm is based on a distance function and a voting function in K-Nearest Neighbors, this algorithm is performed by using a training data set which contains both the input and the target variables. Then the distance of the unknown to the K nearest neighbors determines its class, so that a new item placed in class that has the maximal sum of similarity in the K Nearest Neighbors [13]. In this study, 50% of all data was used for training the KNN algorithm and 3 classes as a group matrix for the KNN classifier. Then we test the classifier with the rest of the data. Classification results are shown in TABLE IV and discussed in result section in detail.

- Multilayer Neural Network(MLP) :

Neural network is a powerful data modeling tool for pattern classification. It is able to capture and represent complicated relationships between inputs and outputs. The most common neural network is the multilayer perceptron (MLP). The MLP neural network is used with 12 neurons in hidden layer and tansigmoid function as activation function and 3 neurons in output layer because we have 3 classes of hemorrhage. Input and targets were selected from feature matrix that was extracted from feature

selection step. This Neural Network is trained using Back Propagation Algorithm with 70% of all data and then with the rest of the data testing the network. Classification Performance results are shown in TABLE V and discussed in result section in detail.

III. EXPERIMENTAL RESULTS:

The real data used in this work was collected from Kashani hospital spiral CT scan, these images are from male and female patients in ages between 15-60 years, which were all collected and labeled by the radiologist. The images that are about EDH, SDH, ICH hemorrhage types and normal brain, are all in jpeg format with 128*128 resolutions.

A. Segmentation Evaluation:

- *Segmentation Evaluation Measures:*

To evaluate the segmentation method used in this study, we compared its outcomes with the doctors' diagnoses (manual method). The following key factors are used in this comparison:

$$sensitivity = \frac{TP}{TP + FN} \times 100 \quad (12)$$

$$specificity = \frac{TN}{TN + FP} \times 100 \quad (13)$$

$$similarity = \frac{2TP}{2TP + FN + FP} \times 100 \quad (14)$$

$$accuracy = \frac{TP + TN}{TP + TN + FP + FN} \times 100 \quad (15)$$

$$BR = \frac{A(XOR)S}{S} \times 100 \quad (16)$$

where, TP describes hemorrhage pixels found by both the proposed segmentation method and manual method, FP describes hemorrhage pixels isolated by the proposed segmentation method but not by the manual method, FN describes hemorrhage pixels isolated by the manual segmentation but not by the proposed segmentation method, and TN describes no hemorrhage pixels found by both methods. In equation (16) BR is the brain hemorrhage detection error, in which A is the hemorrhage area detected and S is the hemorrhage area labeled by physician.

- *Segmentation Results:*

The obtained results in TABLE I demonstrate that the highest error (BR) and the lowest accuracy exist in SDH hemorrhage segmentation. This type of hemorrhage happens in a potentially space (between the dura and the arachnoid), thus the hemorrhage has enough space to expand, which consequently results in very narrow regions that are very near and similar to the skull. This increases the probability of error. Next is the ICH hemorrhage, which is widely known as contusion. Its position is better than the SDH hemorrhage. However, this type does not consist of pure blood; rather it is a combination of various pathologies such as normal brain tissue, crushed brain tissue, edema and blood, therefore it does not have any obvious borders and in some, the hemorrhage regions are scattered throughout the brain. Therefore, it has the second lowest accuracy. The EDH hemorrhage made up of pure blood and has little space to expand (between the dura and the skull), hence it has noticeable borders and its regions, are clearer than other types. Therefore, we were able to segment it with the highest accuracy.

TABLE I. Segmentation results

Type	*Sensitivity (%)*	*Specificity (%)*	*Similarity (%)*	*BR (%)*	*Accuracy (%)*
EDH	93.39	97.23	94.19	45.13	96.22
ICH	90	98.23	91.25	52.17	95.14
SDH	72.41	92.70	65.64	58.24	90.04

TABLE II. Feature Weights obtained by GA

Features	*GA weights*
Area	0.9879
Convex area	0.8358
Filled area	0.8785
Equivdiameter	0.2791
Solidity	0.5689
Perimeter	0.4394
Majoraxislength	0.9442
Minoraxislength	0.3702
Extent	0.5030
Orientation	0.1810
Contrast	0.2237
Correlation	0.4333
Energy	0.6352
Homogeneity	0.6920

B. Feature Selection Results:

As mentioned before, by using the GA based feature selection the best of the 14 features formerly described are selected. To this end, the KNN Classifier is adopted to classify the training data and the resulting error rate is used as the feedback into the feature selection algorithm. The size of the population is 50 and each chromosome contains 14 genes (One gene for each feature), crossover rate is 0.8 and the mutation rate is 0.01. TABLE II contains the features' weights that were obtained by the GA after 50 generations. As seen in this table, among the shape features *area* and *major-axis-length* have the highest weights. Even though, among the texture features *homogeneity* has the highest weight, texture features have low

weights as a whole. This was predictable because only one of the three hemorrhages (ICH) has a different texture (it does not only consist of pure blood like the other two).

C. *Classification Results:*

In this step, the classifiers accuracy before and after the feature selection is compared in TABLE III. Then the results of the KNN and the MLP neural network classifiers are shown in TABLE IV and TABLE V. And later they are compared.

- KNN Classifier Results:

To evaluate the KNN classifier, confusion matrix is used. In this matrix, the diagonal and non-diagonal elements show samples that are correctly and incorrectly classified respectively. TABLE IV shows the KNN confusion matrix. This table displays that by using this classifier only 60% of all images are classified correctly, which is a very low accuracy for medical tasks because this amount of error can be a tremendous threat for the patient's health.

- MLP Classifier Results:

The confusion matrix for the MLP classifier is shown in TABLE V. This table shows that the accuracy of this classifier is 93.3%. In other words, by using this classifier 93.3% of all images are correctly classified and only 7.1% of samples are incorrectly classified. After comparing the results obtained from these tables the MLP classifier has been chosen for the classification purposes.

TABLE III. Classification results before and after feature selection by GA.

Classifiers	***Classifier Accuracy Before Using GA***	***Classifier Accuracy After Using GA***
KNN	53.33%	60%
MLP neural network	86.7%	93.3%

TABLE IV. KNN classifier confusion matrix

	SDH	***EDH***	***ICH***	***Accuracy***
SDH	3	1	1	57.5%
EDH	0	4	1	80%
ICH	2	1	2	43.5%
Accuracy	57.5%	66.66%	50.5%	60%

TABLE V. MLP classifier confusion matrix

	SDH	***EDH***	***ICH***	***Accuracy***
SDH	5	0	0	100%
EDH	0	4	0	100%
ICH	0	1	5	83.3%
Accuracy	100%	80%	100%	93.3%

IV. CONCLUSION

In this paper, an independent and automatic brain hemorrhage segmentation and classification method was proposed. This method was an attempt to improve the accuracy of the physicians' diagnosis and accelerate their decision-making process, which subsequently saves the lives of more patients. To achieve such purposes, an automated segmentation method was proposed in the segmentation step, in which even the smallest hemorrhages were detected. After extracting the features from each detected region and selecting the best of them; in the classification step the hemorrhage regions were classified with two classifiers, from which the neural network classifier's accuracy (93.3%) was higher and therefore more successful than the KNN classifier (60%). Consequently, we could separate the dangerous hemorrhages from others, so in this way treatment process of these patients would be accelerated.

References

[1] Q. Hu, G. Qian, A. Aziz, and W.L. Nowinski, "Segmentation of brain from computed tomography head analysis," in Proceedings of the 27th Annual International Conference of the IEEE-MBS Engineering in Medicine and Biology, vol. 4, pp. 3375–3378, 2005.

[2] A. Lauric, S. Frisken, "Soft segmentation of CT brain data," Technical report, Department of Computer Science, Tufts University, 2007.

[3] S. Loncaric, D. Cosic, and A.P. Dhawan, "Hierarchical segmentation of CT head images," in Proceedings of the 18th Annual International Conference of the IEEE-MBS Engineering in Medicine and Biology, Amsterdam, vol. 2, pp. 736-737, 1996.

[4] D. Kovacenic, S. Loncaric, "CT image labeling using simulated annealing algorithm," Proceedings of the IX European Signal Processing Conference, Greece, vol. 4, pp. 2513-2516, 1998.

[5] R. Maksimovic, S. Stankovic, and D. Milovanovic, "Computed tomography image analyzer: 3D reconstruction and segmentation applying active contour models," International Journal of Medical Informatics, vol. 58, pp. 29-37, september 2000.

[6] M. Mancas, B. Gosselin, "Towards an automatic tumor segmentation using iterative watershed," Proceedings of the Medical Imaging Conference of the International Society for Optical Imaging, vol. 5370, pp.1598-1608, 2004.

[7] S. Manikandan, V. Rajamani, "A mathematical approach for feature selection and image retrieval of ultrasound kidney image databases," European Journal of Scientific Research, vol. 24, pp. 163–171, 2008.

[8] H. Shao, H. Zhao, "Automatic analysis of the skull based on image content.," Third International Symposium on Multispectral Image Processing, china, vol. 5286, pp.741-746, october 2003.

[9] J. Wasserberg, B. Mitchell, CT scan guideline, Dept Neurosurgery, University of Birmingham, Oct 2009.

[10] P. Maduskar, M. Acharyya, "Automatic identification of intracranial hemorrhage in non-contrast CT with large slice thickness for trauma cases," Proceedings of the SPIE, vol. 7260, pp 8-13, 2009.

[11] A. Kharrat, K. Gasmi, M. Ben Messaoud, N. Benamrane, and M. Abid, "A Hybrid Approach for Automatic Classification of Brain MRI Using Genetic Algorithm and Support Vector Machine," Leonardo Journal of Sciences, vol. 9, pp. 71-82, 2010.

[12] Y. Cheng-Huei, Ch. Li-Yeh, and Y. Cheng-Hong, "A Hybrid Filter/Wrapper Method for Feature Selection of Microarray Data," Journal of Medical and Biological Engineering, Vol. 30, No. 1,pp. 23-28, 2010.

[13] R. J. Ramteke, Y. Khachane Monali," Automatic Medical Image Classification and Abnormality Detection Using K-Nearest Neighbour," International Journal of Advanced Computer Research, vol. 2, No. 4, December 2012.